AHM
Archives of Hand and Microsurgery

Original Article

pISSN 2586-3290 · eISSN 2586-3533
Arch Hand Microsurg 2022;27(2):125-133
https://doi.org/10.12790/ahm.21.0148

Received: December 3, 2021
Revised: February 3, 2022
Accepted: February 11, 2022

Corresponding author:
Chang-Hun Lee
Department of Orthopedic Surgery,
Hanyang University College of Medicine,
222-1 Wangsimni-ro, Seongdong-gu,
Seoul 04763, Korea
Tel: +82-2-2290-8485
Fax: +82-2-2290-3774
E-mail: drlch79@hanyang.ac.kr
ORCID:
https://orcid.org/0000-0003-4330-7726

*Young Seok Lee and Heaseong Jeoung contributed equally to this study as co-first author.

Comparative finite element analysis of an osseointegration system in transradial amputation: a proposal of a new design for osseointegration

Young Seok Lee[1,*], Heaseong Jeoung[2,*], Seung Gun Lee[3], Dong-Hong Kim[3], Chang-Hun Lee[3]

[1]Department of Orthopedic Surgery, Hanyang University Guri Hospital, Guri, Korea
[2]Machine Dynamics Laboratory, Department of Mechanical Engineering, Hanyang University, Ansan, Korea
[3]Department of Orthopedic Surgery, Hanyang University College of Medicine, Seoul, Korea

Purpose: Conventional osseointegration systems have been applied in patients requiring transhumeral or transfemoral amputation. However, the application of these systems to transradial amputation is limited by the small diameter of the radius and ulna. Our study compared the biomechanical stability of a novel osseointegration system with that of a conventional system used in transradial amputation through an analysis of finite element (FE) models.

Methods: We established three-dimensional FE models of transradial amputations, which were osseointegrated with both the novel and conventional systems. External loads were applied to the FE models with compressive force and tensile force along the long axis, horizontal shear force, and vertical shear force. The maximum equivalent stress (MES) and the distribution of stress through the radius and ulna were evaluated.

Results: The MES of the radius and ulna was higher in the conventional system when compressive, tensile, and vertical shear forces were applied. However, when a horizontal shear force was applied, the opposite result was found. The distribution of stress was more effective in the novel system.

Conclusion: Three-dimensional FE modeling showed that the novel system enabled a lower stress level and a more even distribution of stress for osseointegration in transradial amputation.

Keywords: Finite element analysis, Transradial amputation, Osseointegration

Introduction

Transradial amputation may result from a congenital condition, trauma, infection, or tumor [1]. In the cases of upper-extremity amputations, trauma is the leading cause, accounting for 80% of acquired amputations and occurring most often in men aged 15 to 45 years. Meanwhile, the second most prevalent cause is tumor and vascular complications of diseases [2]. In the United States, the prevalence of amputations was 1.6 million in 2005, with projections suggesting this prevalence may double by the year 2050 [3].

The upper extremities are highly complex limbs with neurovascular bundles, lymphatics, muscles, and bones that come together to form a functional appendage used during daily activities [2]. As such, the loss of the wrist and/or hand leads to functional and psychological problems. Depending upon the level of amputation, various clinical considerations exist; ultimately, the goal in any amputa-

tion is to save all viable tissue as this directly correlates with improved functional status [4,5]. Lee et al. [6] reported that close proximity of the amputation site to the elbow significantly decreased residual function, including forearm rotational movement. Therefore, it is important to preserve the length of the radius as much as possible.

Currently, only a few osseointegrated transcutaneous prosthetic systems (such as OPRA system [Integrum AB, Mölndal, Sweden] and ITAP system [Stanmore Medical Group, Stevenage, UK]) for use in humans exist but none are approved for general use in the United States [7,8]. Conventional osseointegration systems have been applied to transhumeral (OPRA system and ITAP system) and transfemoral amputations (OPRA system and ISP Endo/Exo prosthesis [ESKA Implants AG, Lubeck, Germany]). However, the application of these systems in patients requiring transradial amputations has limitations due to the small diameter of the radius and ulna. The average intramedullary canal diameter of the humerus is 14.5 mm (range, 9.4–20.5 mm) [9], while the average diameter of the medullary cavity of the distal shaft of the radius is 6.7 mm (range, 6.1–7.3 mm) and the minimum diameter of the ulna medullary cavity is 4.2 mm (range, 2.0–6.7 mm) [10,11].

In a review of the literature, no biomechanical study about osseointegrated implants for the transradial amputee was found. Because major upper-extremity amputees account for only 8% of the 1.5 million individuals living with limb loss [3] and upper-extremity loss does not affect weight-bearing [11]; therefore, the importance of upper-extremity amputation is lowered. In addition, it is important to recover the fine-movement capacity of the upper extremity, especially the hand and wrist, so it is considered to be because the difficulty is higher than that of the lower-extremity reconstruction. Applying a small implant with the same design as the conventional system can increase the risk of periprosthetic fracture due to stress concentration in the forearm bone. Through these points, the need for a new design for osseointegration in the forearm bones has emerged.

From these points, we made a new design implant with several modifications. And in a similar way to Kaku et al. [12] and Liu et al. [13], our study aimed to evaluate the stress-distribution pattern and biomechanical stability of a novel osseointegration system and to compare it with that of the conventional system in transradial amputation using a finite element (FE) model. The FE model is a mature, validated technique based on three-dimensional (3D) computed tomography (CT) datasets that integrate structure to estimate bone strength under various loading conditions and is increasingly helpful in the preclinical testing of orthopedic areas [14]. The FE model divides the target into a finite number of small elements and enables precise prediction and analysis of situations through computer modeling. We hypothesized that the novel system would reduce the stress intensity and more evenly distribute stress loading throughout the radius and ulna.

Methods

Ethics statement: This study was conducted after obtaining approval from the Institutional Review Board of Hanyang University Hospital (No. 2020-07-017). We obtained informed consent from the patient.

1. Finite element modeling

We established 3D FE models of transradial amputations, which were osseointegrated with novel and conventional systems. We used the Ansys Workbench ver. 17.0 software program (Ansys Inc., Canonsburg, PA, USA) to create FE models. Two FE models were created, one representing a transradial amputation with a conventional osseointegration implant and the other representing the same forearm bones with a novel osseointegration implant. The geometry of the forearm bones was acquired from CT scans (slice thickness, 1 mm) of a 34-year-old male patient's forearm bones. For reading CT data, an open-source software (InVesalius) was used, and the computer-aided design exchange program was used to convert CT data into 3D remodeling format files. Because the implant had to be newly designed according to the curvature of the radius and ulna, Vascular Modeling Toolkit program was used to extract the centerline of the shape with curvature. The main cause of transradial amputation is trauma (up to 80%), which occurs in young men (aged 15–45 years) [2], so we set the FE model to incorporate the normal bone mineral density of a typical young man. The amputated radius and ulna model represented the most functional osteotomy level of 18cm below the olecranon tip [6]. The surface-shape contours of the two implants were fitted in both forearm bones and implemented into the FE models. In this process, we designed the FE model under two conditions. First, the implants with the same outer diameter of the intramedullary part were assumed to be in close contact with the bone. Second, the implant and bone were bonded to represent full osseointegration. For FE models analysis, Ansys program was used, and only default values were used.

https://doi.org/10.12790/ahm.21.0148

2. Material properties

The FE model was fixed at the end of the amputation level of the radius and ulna and the interface between the implant and bone was modeled as a continuous bond. This arrangement implies ideal osseointegration was achieved without any relative motion at the interface. In other words, the implant was rigidly anchored in the bone, showing a fixed and similar type of bond at all prosthesis material interfaces. And we set the proximal end of the radius and ulna as a fixed condition. The biomechanical properties of the radius and ulna bones were composed of cortical bone and cancellous bone. The setting values are described in Table 1. And for the implant properties, we used the properties of titanium alloy provided by Ansys.

3. Loading conditions and measurements

External loads were applied to the FE models with compressive and tensile forces measuring 60 N along the long axis (Z-axis). Horizontal shear force (X-axis) and vertical shear force (Y-axis) to the FE models were similarly applied at a strength of 60 N. Various external loads have been applied in biomechanical studies on the forearm. We assumed that 60 N is the appropriate size for transradial amputee referring to Santoni et al.'s study [15]. Previous studies showed horizontal shear force is a force assuming a stress situation that occurs when radial and ulnar deviation movements occur in the wrist. Vertical shear force is a force assuming a stress situation that occurs during flexion and extension movements in the wrist and elbow. The maximum equivalent stress around integrated implants in the radius and ulna was calculated. Also, the stress-distribution pattern of the load applied to the whole length of the radius and ulna was evaluated in three sections (Fig. 1). All experiments were performed in accordance with relevant named guidelines and regulations.

Table 1. Bone material properties

Material property	Cortical bone	Cancellous bone
Young's modulus (MPa)		
X direction	6,900	680
Y direction	8,500	1,210
Z direction	18,400	2,050
Poisson's ratio		
XY	0.42	0.14
YZ	0.31	0.10
XZ	0.32	0.11
Shear modulus (MPa)		
XY	2,400	330
YZ	4,900	600
XZ	3,600	400

4. Implant design

Currently, there is no osseointegration system commercially available for transradial amputees. However, there have already been some tests to apply the existing osseointegration system modeled after the shape of a transhumeral or transfemoral implant applied in clinical cases. The conventional osseointegration system incorporates three main components: a threaded titanium implant (the fixture), a skin-penetrating cylindrical implant (the abutment), and a titanium screw (the abutment screw) [16]. A new implant was designed by modifying several points in the conventional osseointegration system (Fig. 2); specifically, we designed to allow proximal screw fixation to achieve initial rotational stability in the novel osseointegration system. The surface of the implant was treated with a porous coating so that bony ingrowth could occur better in the distal part of the implant, while a longitudinal groove was devised to increase the contact area. In addition, the radius and ulna have a slight curvature (bowing); so, to reduce the occurrence of iatrogenic damage such as cortical breakage or fracture. And the diameter of the implant's middle area was designed smaller so as to be more easily bent, facilitating greater adaptation during the implant-insertion process. Finally, the stem was designed to be longer to reduce the stress concentration at the proximal end of the integrated implant and to distribute the stress more broadly throughout the radius and ulna.

Results

When a loading force of 60 N was applied on the implant along the Y-axis (vertical shear force) and the Z-axis (compressive and tensile force), the maximum equivalent stress was higher in the conventional model rather than in the novel model except for in section 3 of the ulna. However, when a horizontal shear force of 60 N was applied (X-axis), the novel system received more stress than the conventional system in sections 2 and 3 of the radius and sections 1 and 2 of the ulna (Table 2).

The stress at the proximal radius and ulnar shaft was decreased in the novel system when stress was loaded along the X-axis (horizontal shear), while that at the shaft of the radius was increased in the novel system condition (Fig. 3). When stress was loaded along the Y-axis (vertical shear force), the stress concentration throughout the radius was decreased in the novel system (Fig. 4). Finally, when stress was applied along the Z-axis (compressive and tensile forces), the stress concentration throughout the radius and ulna was decreased in the

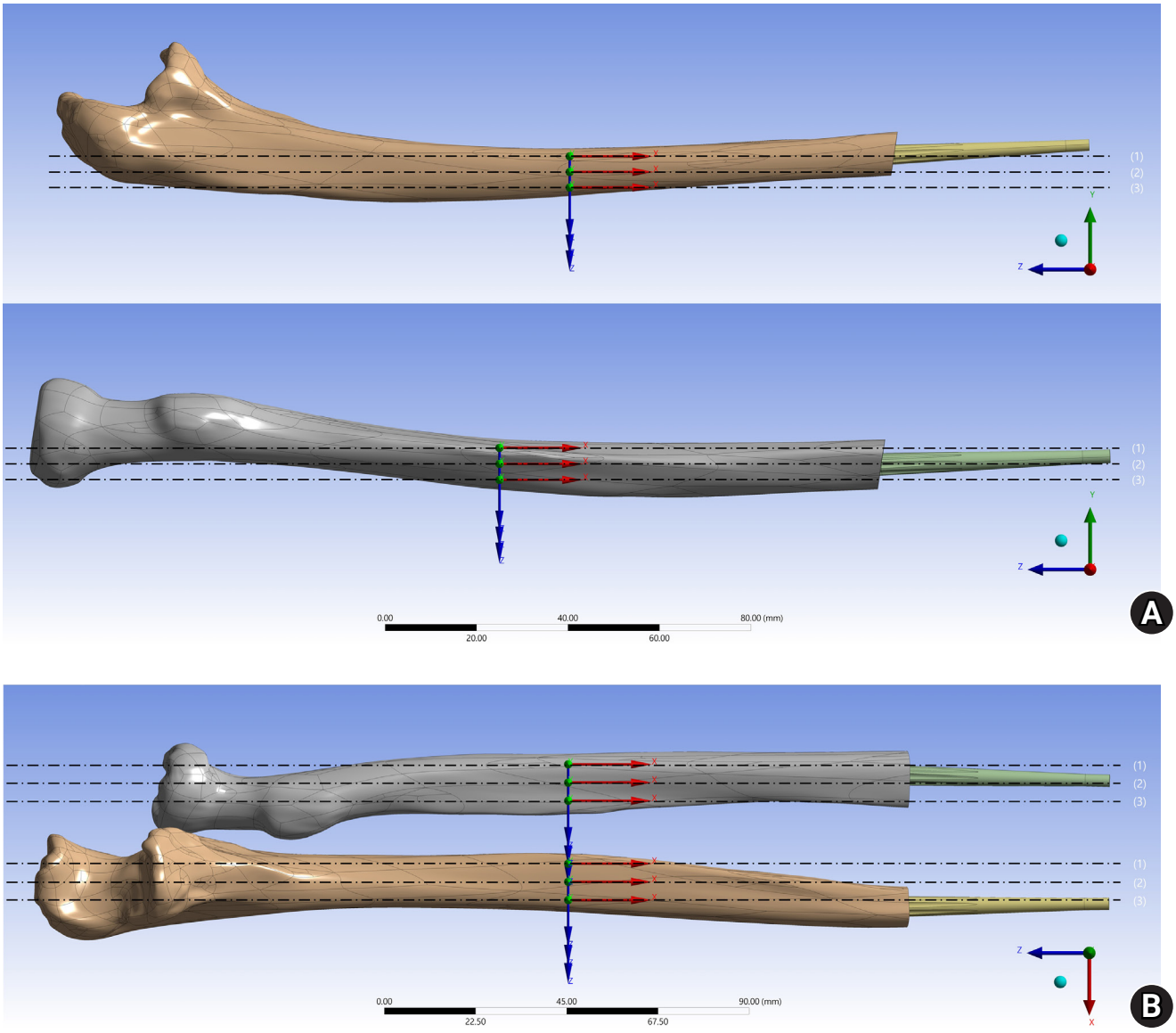

Fig. 1. The stress-distribution pattern and maximum equivalent stress were evaluated in each of the three sections (1, 2, 3) below: (A) X-axis and (B) Y and Z-axis.

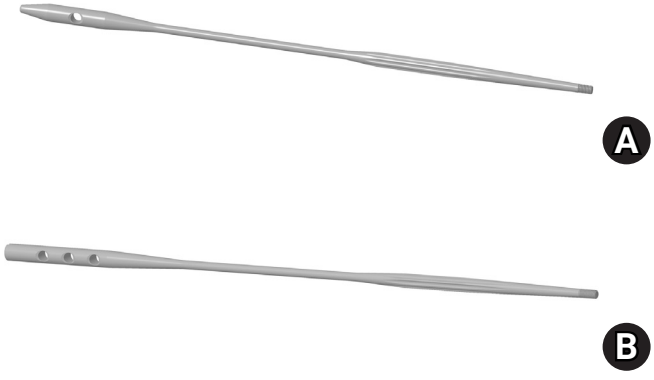

Fig. 2. The new upper-extremity implant design assessed in this study. (A) Radius implant and (B) ulnar implant.

novel system (Fig. 5).

Discussion

Patients with amputated limbs have traditionally relied on a stump-socket interface for prosthetic attachment [7]. This type of prosthetic design is associated with several problems, such as skin changes, increased energy expenditure during ambulation, and disuse osteopenia [17-19]. Several types of osseointegration systems have been developed to overcome these problems and are currently clinically available; however, these osseointegration systems also encountered several problems of their

https://doi.org/10.12790/ahm.21.0148

Table 2. Maximum equivalent stress at each section after application of an external load (60 N) along each axis

External load (60 N) application along the axis		Section 1	Section 2	Section 3
X-axis				
Conventional system	Radius	29.123	32.484	13.027
	Ulna	39.335	22.351	17.008
Novel system	Radius	24.194	42.453	14.63
	Ulna	104.09	28.816	16.03
Y-axis				
Conventional system	Radius	52.21	31.281	27.361
	Ulna	15.329	23.733	21.674
Novel system	Radius	49.414	30.366	25.523
	Ulna	14.38	22.581	57.157
Z-axis				
Conventional system	Radius	1.3949	1.9997	1.1668
	Ulna	1.1521	1.1741	3.0583
Novel system	Radius	0.95711	1.593	0.76815
	Ulna	0.75936	1.0219	3.9029

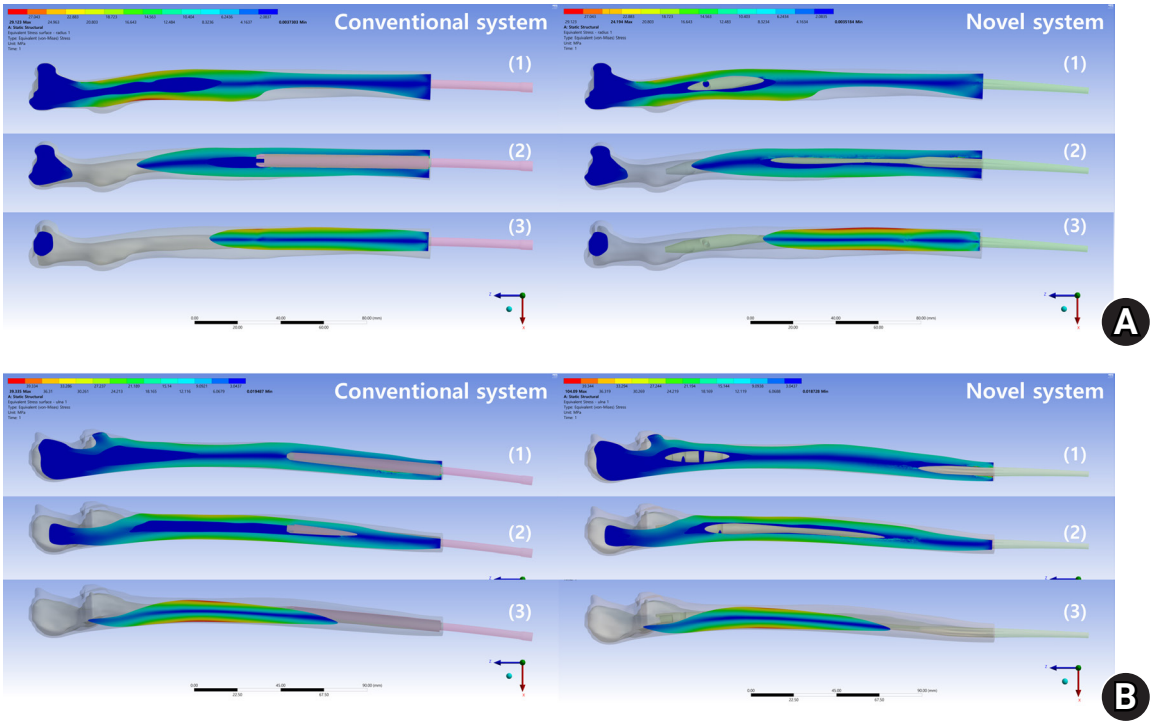

Fig. 3. Stress-distribution pattern when stress was loaded along the X-axis at the radius (A) and the ulna (B).

own, which are infection, periprosthetic bone fracture, bone loss due to stress shielding, and implant failure [20,21]. Furthermore, we are concerned that the conventional design available for transhumeral and transfemoral amputees is not suitable for the transradial amputee. Specifically, the short length of the conventional system inserted into a long bone with a small diameter increases the risk of periprosthetic fracture due to targeted stress concentration.

Osseointegrated implants are exposed to daily activities, consisting of flexion, extension, supination, and pronation of the elbow and radial deviation and ulnar deviation of the wrist. Our study showed that, when subjected to horizontal shear force, the radius and ulna received higher maximum equivalent stress in the novel system. In contrast, with compressive, ten-

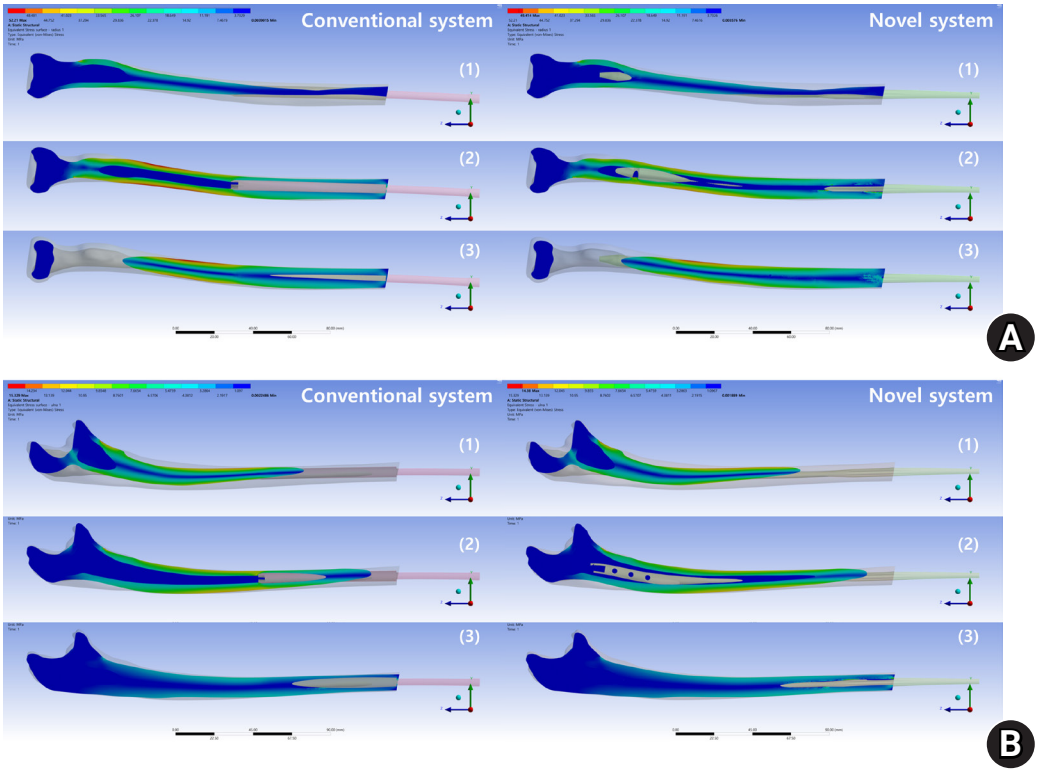

Fig. 4. Stress-distribution pattern when stress was loaded along the Y-axis at the radius (A) and the ulna (B).

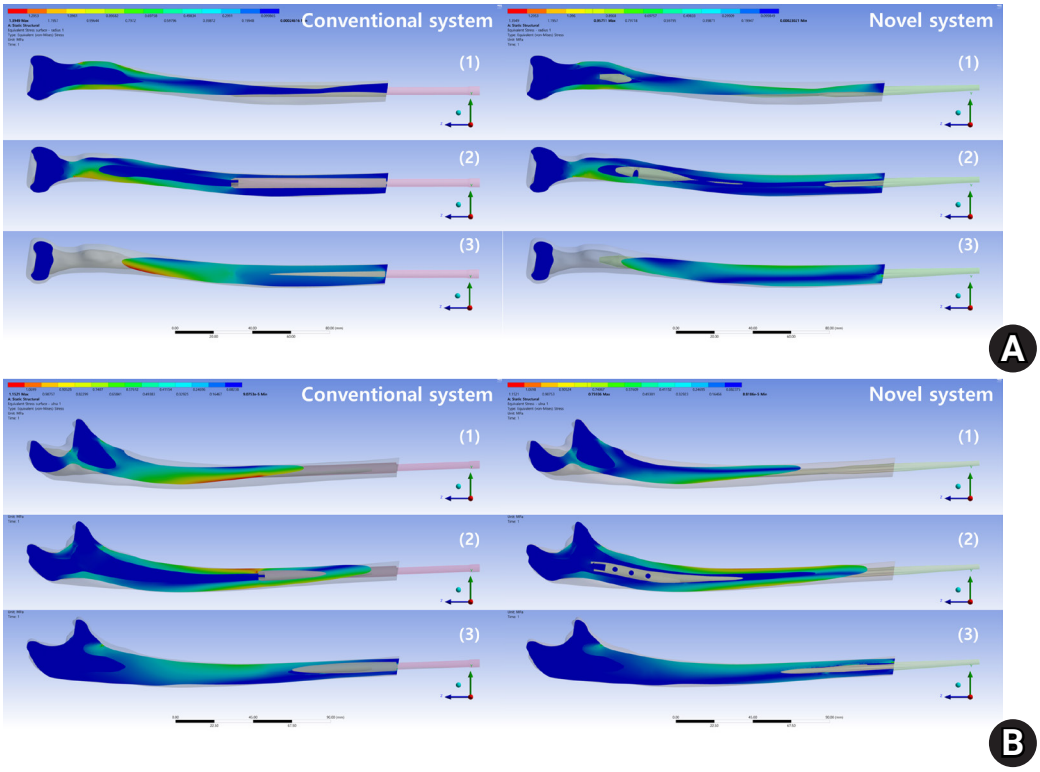

Fig. 5. Stress-distribution pattern when stress was loaded along the Z-axis at the radius (A) and the ulna (B).

https://doi.org/10.12790/ahm.21.0148

sile, and vertical shear forces, the radius and ulna received lower maximum equivalent stress in the novel system. Thus, more even stress distribution throughout the radius and ulna was observed in the novel system. The stress loaded along the X-axis (horizontal shear force) is assumed to be that loaded during radial and ulna deviation of the wrist, while the stress loaded along the Y-axis (vertical shear force) is assumed to be the force loaded during flexion and extension of the elbow and wrist. Compressive and tensile forces along the Z-axis are assumed to be the result of longitudinal movements characterized by changes in ulnar variance relative to the radial corner during forearm supination and pronation.

The novel system has a long stem, sharing the characteristic of an intramedullary nail. Osseointegration through the whole length of the radius and ulna was supposed to evenly distribute stress transferred from the distal end of the implants. Ding et al. [22] reported that increasing the diameter and length of the implant decreased the stress and strain on the alveolar crest per biomechanical analysis of high-quality FE models of complete range mandibles. Baggi et al. [23] also reported the influence of implant diameter and length on the stress distribution of osseointegrated implants related to crestal bone geometry. Stress values and concentration areas are decreased for cortical bone when the implant diameter is increased, whereas more effective stress distributions for cancellous bone were observed with increasing implant length [23]. In the case of transradial amputation, the medullary diameter of the radius and ulna is not a modifiable factor, but the length of the implant is. The results of our study were consistent with those of previous studies in that the implant length affected the stress distribution and maximum equivalent stress.

Despite our good results, two problems of the novel system were recognized during FE analysis. First, the maximum equivalent stress of the radius and ulna in the horizontal shear force was higher in the novel system. Also, the stress distribution in section 3 of the ulna in the novel system was definitely less effective than that seen with the conventional system. Notably, the radius can experience physiologic bowing in the horizontal plane [24], and adaptation to this physiologic bowing by deep insertion of the long stem seems to be the cause of greater maximum equivalent stress. In the implant design, the diameter of shaft of the novel radial implant was 3.0 mm (supplement). To decrease the stress value in relation to horizontal force, a larger radial-implant diameter can be considered. Also, increased stress around the distal longitudinal grooves of both the radius and ulna implants was observed. There is a tendency to increase the stress value in the angled location rather than the cylindrical or smooth location in FE analysis. According to Xiaobin and Zelong [25], when the surfaces are angled, the stress concentration is large when forces are applied from multiple directions. Conversely, when the surfaces were rounded, it was found that the stress concentration was relatively low for the same external forces. For clinical application of the implants, a cylindrical design rather than an angular groove modality might reduce bone absorption in the insert area.

Stenlund et al. [26] found that the elastic strains and principal compressive stresses in the bone in direct contact with the abutment at the most distal location may indicate unfavorable bone remodeling, resulting in a decrease in bone density with time. Meanwhile, Nebergall et al. [20] reported that the transmission of loads to the contact point between the bone and implant can cause cortical thinning or bone resorption. This results a high risk of loosening of that area, together with various complications in the distal portion, including implant loosening and periprosthetic fractures. Ultimately, the need for reoperation to replace the entire implant will increase [27].

Our study has some limitations. First, there was a lack of simulation of the anisotropic material properties of human bone. Although the FE model was designed by distinguishing the material properties of cortical and cancellous bone, this does not fully reflect the material properties of human bone. Moreover, the amputated site may present a combination of damaged bone, callus, hematoma, and fibrotic tissues. Additional analysis is likely required in future research, incorporating detailed simulation of a more realistic bone model and some clinical cases. Second, it should be realized that this loading configuration does not represent a whole transradial amputation case. When applied in clinical practice, amputation levels and the loss of soft tissue including muscles vary between patients. Thus, these findings should be generalized with caution and unexpected disadvantages of the model can be found. Sufficient research is needed, including cadaver research before clinical application. Despite these limitations, however, we investigated the biomechanical properties of the novel and conventional implants for the transradial amputee and confirmed the chance of improvement of osseointegration in the forearm bone.

In conclusion, 3D FE models showed that the design of a novel system provides a lower stress level and more even stress distribution for osseointegration in transradial amputation. This novel osseointegration system is expected to reduce complications such as periprosthetic fracture and implant failure and to improve long-term implant survival.

ORCID

Young Seok Lee, https://orcid.org/0000-0002-0217-2661
Heaseong Jeoung, https://orcid.org/0000-0003-4894-7087
Seung Gun Lee, https://orcid.org/0000-0001-7401-7620
Dong-Hong Kim, https://orcid.org/0000-0002-9088-7551
Chang-Hun Lee, https://orcid.org/0000-0003-4330-7726

Conflicts of interest

The authors have nothing to disclose.

Funding

This work was supported by the National Research Foundation of Korea (NRF) grant funded by the Korea government (MSIT) (No. 2020R1A2C2101353) and the research fund of Hanyang University (HY-202000000000506).

References

1. Amornvit P, Rokaya D, Keawcharoen K, Thongpulsawasdi N. Stress distribution in implant retained finger prosthesis: a finite element study. J Clin Diagn Res. 2013;7:2851-4.
2. Maduri P, Akhondi H. Upper limb amputation [updated 2021 Aug 12]. In: StatPearls [Internet]. Treasure Island (FL): StatPearls Publishing; 2022 [cited 2021 Dec 3]. Available from: https://www.ncbi.nlm.nih.gov/books/NBK540962/.
3. Ziegler-Graham K, MacKenzie EJ, Ephraim PL, Travison TG, Brookmeyer R. Estimating the prevalence of limb loss in the United States: 2005 to 2050. Arch Phys Med Rehabil. 2008;89:422-9.
4. Atroshi I, Rosberg HE. Epidemiology of amputations and severe injuries of the hand. Hand Clin. 2001;17:343-50.
5. Dillingham TR, Pezzin LE, MacKenzie EJ. Limb amputation and limb deficiency: epidemiology and recent trends in the United States. South Med J. 2002;95:875-83.
6. Lee G, Kim SJ, Ha JH, Lee CH, Choi YJ, Lee KH. Residual rotation of forearm amputation: cadaveric study. BMC Musculoskelet Disord. 2020;21:40.
7. Grisez BT, Hanselman AE, Boukhemis KW, Lalli TA, Lindsey BA. Osseointegrated transcutaneous device for amputees: a pilot large animal model. Adv Orthop. 2018;2018:4625967.
8. Tomaszewski PK, van Diest M, Bulstra SK, Verdonschot N, Verkerke GJ. Numerical analysis of an osseointegrated prosthesis fixation with reduced bone failure risk and periprosthetic bone loss. J Biomech. 2012;45:1875-80.
9. Barth J, Garret J, Boutsiadis A, et al. Is global humeral head offset related to intramedullary canal width?: a computer tomography morphometric study. J Exp Orthop. 2018;5:35.
10. Hopf JC, Jähnig A, Jorg T, Westphal RS, Wagner D, Rommens PM. Computer tomographic analysis of anatomic characteristics of the ulna: essential parameters for preshaped implants. PLoS One. 2020;15:e0232988.
11. Pierrie SN, Gaston RG, Loeffler BJ. Current concepts in upper-extremity amputation. J Hand Surg Am. 2018;43:657-67.
12. Kaku N, Tanaka A, Tagomori H, Tsumura H. Finite element analysis of stress distribution in flat and elevated-rim polyethylene acetabular liners. Clin Orthop Surg. 2020;12:291-7.
13. Liu HC, Jiang JS, Lin CL. Biomechanical investigation of a novel hybrid dorsal double plating for distal radius fractures by integrating topology optimization and finite element analysis. Injury. 2020;51:1271-80.
14. Engelke K, Libanati C, Fuerst T, Zysset P, Genant HK. Advanced CT based in vivo methods for the assessment of bone density, structure, and strength. Curr Osteoporos Rep. 2013;11:246-55.
15. Santoni BG, Aira JR, Diaz MA, Kyle Stoops T, Simon P. Radiographic evaluation of acute distal radius fracture stability: a comparative cadaveric study between a thermo-formable bracing system and traditional fiberglass casting. Clin Biomech (Bristol, Avon). 2017;47:20-6.
16. Jönsson S, Caine-Winterberger K, Brånemark R. Osseointegration amputation prostheses on the upper limbs: methods, prosthetics and rehabilitation. Prosthet Orthot Int. 2011;35:190-200.
17. Dudek NL, Marks MB, Marshall SC, Chardon JP. Dermatologic conditions associated with use of a lower-extremity prosthesis. Arch Phys Med Rehabil. 2005;86:659-63.
18. Meulenbelt HE, Geertzen JH, Jonkman MF, Dijkstra PU. Skin problems of the stump in lower limb amputees: 1. A clinical study. Acta Derm Venereol. 2011;91:173-7.
19. Waters RL, Mulroy S. The energy expenditure of normal and pathologic gait. Gait Posture. 1999;9:207-31.
20. Nebergall A, Bragdon C, Antonellis A, Kärrholm J, Brånemark R, Malchau H. Stable fixation of an osseointegated implant system for above-the-knee amputees: titel RSA and radiographic evaluation of migration and bone remodeling in 55 cases. Acta Orthop. 2012;83:121-8.
21. Tillander J, Hagberg K, Hagberg L, Brånemark R. Osseointegrated titanium implants for limb prostheses attachments: infectious complications. Clin Orthop Relat Res. 2010;468:2781-8.
22. Ding X, Liao SH, Zhu XH, Zhang XH, Zhang L. Effect of di-

ameter and length on stress distribution of the alveolar crest around immediate loading implants. Clin Implant Dent Relat Res. 2009;11:279-87.
23. Baggi L, Cappelloni I, Di Girolamo M, Maceri F, Vairo G. The influence of implant diameter and length on stress distribution of osseointegrated implants related to crestal bone geometry: a three-dimensional finite element analysis. J Prosthet Dent. 2008;100:422-31.
24. Firl M, Wünsch L. Measurement of bowing of the radius. J Bone Joint Surg Br. 2004;86:1047-9.
25. Xiaobin LP, Zelong L. Stress concentration factors due to typical geometric discontinuities for shaft design by numerical simulation. Paper presented at 2013 ASEE Annual Conference & Exposition; 2013 Jun 23-26; Atlanta, GA. Atlanta, GA. ASEE. 2013.
26. Stenlund P, Trobos M, Lausmaa J, Brånemark R, Thomsen P, Palmquist A. Effect of load on the bone around bone-anchored amputation prostheses. J Orthop Res. 2017;35:1113-22.
27. Al Muderis M, Khemka A, Lord SJ, Van de Meent H, Frölke JP. Safety of osseointegrated implants for transfemoral amputees: a two-center prospective cohort study. J Bone Joint Surg Am. 2016;98:900-9.